Superstable phenomena of 1-D map with a trapping window and its application

Yusuke Matsuoka[†] and Toshimichi Saito[†]

†EECE Dept., HOSEI Univ., 3-7-2 Kajino-cho, Koganei-shi, Tokyo, 184-8584 Japan
Email: {matsuoka@nonlinear.k., tsaito@ } hosei.ac.jp

Abstract—This paper studies dynamics of 1-D maps with a trapping window. The window can change chaotic or quasi-periodic orbits of original 1-D maps into various superstable phenomena. Using some examples of piecewise linear systems, we analyze dynamics precisely. Application to A/D converters is also discussed.

1. Introduction

This paper studies dynamics of 1-D maps with a trapping window (ab. TWmaps). When an 1D map exhibits torus or chaos, the window can change it into complex superstable periodic orbit (ab. SSPO) [1]- [5]. The SSPO has interesting properties : superstable for initial state, very fast transient to stable steady state and sensitivity for parameter perturbation. There exist complicated bifurcation phenomena of rich SSPOs [3] and their analysis is pretty hard. Such TWmaps appear in some practical systems : chaos control systems [5], sigma-delta modulators with a trapping window [6], a simplified model of power converters [7], a B-Z map with noise-induced order [8]-[9] and so on. Analysis of TWmap and SSPOs are important to approach new bifurcation theory and provides basic information for design of practical systems.

This paper studies the 1D TWmaps and related applications. First, we overview the TWmaps with SSPOs. Second, we study an example of the TWmaps : a circle map with the window. If the window does not present the map exhibits periodic behavior or torus. We then investigate effects of the parameter on the window and clarify interesting bifurcation: as the slope decreases to zero, the torus can change into complicated SSPO; as the slope increases, the torus can change into various chaotic behavior.

Third, we consider an application of 1-D TWmap to analog-to-digital converters (ab. ADCs). Dynamics of the circle map is related closely to that of basic ADC [10], [11]. Adding a zero-slope window to the circle map, resolution and robustness can be improved dramatically. Note that we have discussed 1-D TWmap in [1], however effects of parameter(s) of the window have not been discussed sufficiently.
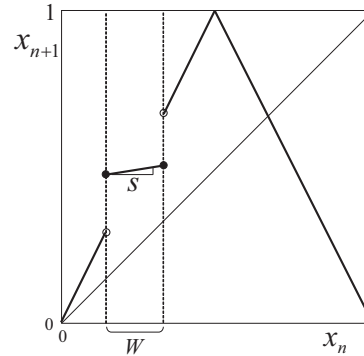

Figure 1: Feature of 1-D TWmap.

2. 1-D maps with a trapping window

We consider the TWmaps as shown in Fig. 1 :

$$x_{n+1} \equiv F(x_n) = \begin{cases} f_1(x_n) & \text{for } x_n \notin W \\ sx_n + h & \text{for } x_n \in W, \end{cases} \quad (1)$$

where $x_n \in I_1$ is a state variable, $0 \le h \le 1$, $I_1 \equiv [0, 1]$ and n denotes discrete time. f_1 and F are maps from I_1 to itself. $W \subset I_1$ represents a trapping window having a slope s. Typical maps are shown in Fig. 2.

If a width of the window $|W| = 0$, the map exhibits chaos when f_1 is the tent map as shown in Fig. 2 (c).

If $|W| \ne 0$ and $s = 0$ as shown in Fig. 2 (b) and (d), the orbits can be changed into SSPOs [5], [1].

If $|W| \ne 0$ and $s \ne 0$, the TWmaps exhibit periodic and chaotic phenomena and various bifurcations as shown in Section 3. Hereafter, we focus on the case where f_1 is equivalent to the circle map such as Fig. 2 (b). Note that dynamics of the circle map is related to some practical systems such as ADCs [6] and PLLs [12].

3. A circle map with a trapping window

We show objective TWmap in Fig. 3 and consider its dynamics. Fig. 3 is referred to as a circle TWmap and is
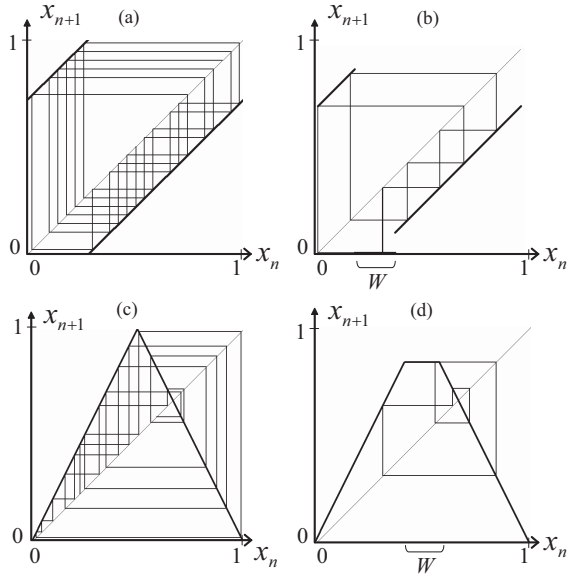
Figure 2: Typical behavior of 1-D maps. (a) Torus, (b) SSPO in a TWmap based on circle map, (c) Chaos, (d) SSPO in a TWmap based on chaotic map.
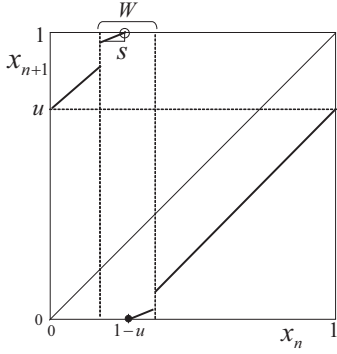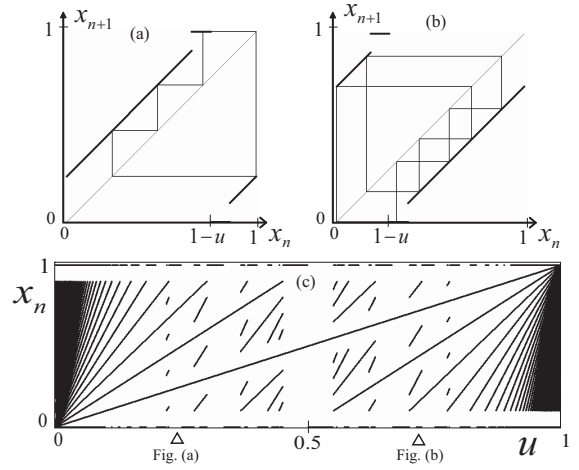

Figure 3: Feature of the circle TWmap.

Figure 4: Typical phenomena of the circle TWmap for $s = 0$ and $\epsilon = 0.1$. (a) SSPO for $u = 0.24$, (b) SSPO for $u = 0.72$, (c) A bifurcation diagram. All the orbits are SSPOs.
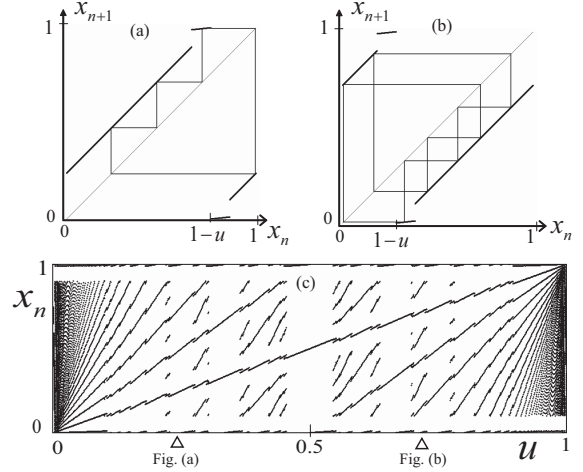

Figure 5: Typical phenomena of the TWmap for $s = 0.1$ and $\epsilon = 0.1$. (a) Periodic orbit for $u = 0.24$, (b) Periodic orbit for $u = 0.72$, (c) A bifurcation diagram.

described by

$$x_{n+1} = F(x_n) = \begin{cases} x_n - Q(x_n) + u & \text{for } x_n \notin W \\ sx_n - Q(x_n) + u & \text{for } x_n \in W, \end{cases}$$

$$y_n \equiv Q(x_n) = \begin{cases} 1 & \text{for } x_n \geq x_c \\ 0 & \text{for } x_n < x_c, \end{cases} \quad (2)$$

where $u \in [0, 1]$ is a control parameter and x_c is the center of W. Let $W \equiv [x_c - \epsilon, x_c + \epsilon]$. ϵ denotes a half width of the window. For simplicity, we assume $0 \leq \epsilon < 0.5$ and $0 \leq s < \frac{1}{\epsilon}$ where $x_c \equiv 1 - u$. As a preparation, we describe the case where the window does not present. In this case, Eq. (2) is equivalent to the circle map. u corresponds to the rotation number and the TWmap exhibits periodic and quasi-periodic orbits for rational and irrational rotation numbers, respectively.

First, we consider the case of $|W| \neq 0$ and $s = 0$. The TWmap has a zero slope on the window as shown in Fig. 4 (a) and (b). We can see that periodic/quasi-periodic orbits (torus) for $|W| = 0$ (see Fig. 2 (a)) can be changed into various SSPOs. If Eq. (3) is satisfied, the orbit is said to be SSPO with period k [3].

$$F^k(x_{sp}) = x_{sp}, \; F^j(x_{sp}) \neq x_{sp}, \; \frac{d}{dx_n}F^k(x_{sp}) = 0, \quad (3)$$

where $0 < j < k$ is a positive integer and j does not exist if $k = 1$. Fig. 4 (c) shows a bifurcation diagram. All the orbits can hit the window and a variety of SSPOs exist. In order to characterize phenomena, we then define a frequency ratio :
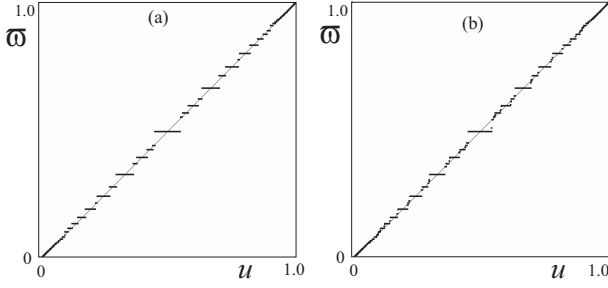
$$\omega = \frac{1}{N} \sum_{n=1}^{N} y_n, \quad (4)$$

- 56 -

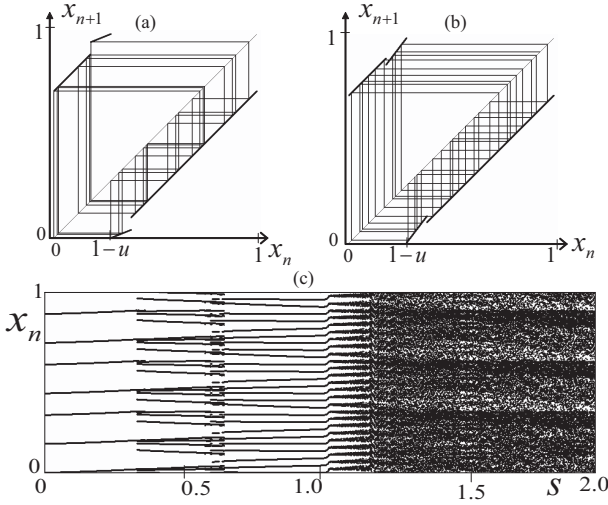Figure 6: Characteristics of a frequency ratio ω for $\epsilon = 0.1$. (a) $s = 0$, (b) $s = 0.1$.

Figure 7: Typical phenomena of the TWmap for $\epsilon = 0.1$ and $u = 0.72$. (a) Periodic orbit for $s = 0.4$, (b) Chaos for $s = 1.3$, (c) A bifurcation diagram.

where N is a sufficiently large integer. ω represents a ratio of output 1 of $Q(x_n)$ per a period. Characteristics of ω for u is shown in Fig. 6 (a) which forms incomplete devil's stair case.

Second, we consider the case of $0 < s < \frac{1}{\epsilon}$. The slope on the window of Eq. (2) is non-zero and the map has three parameters ϵ, u and s. Note that we assume $F(x_n)$ is modulus 1 if $F(x_n) > 1$ or $F(x_n) < 0$. Fig. 5 shows typical phenomena of the TWmap. The orbits and bifurcation diagram are similar to that for $s = 0$ in Fig. 4. In the TWmap, the slope is s on the window and is 1 otherwise. That is, if $0 < s < 1$, an orbit is stable if it passes through W. It means that the circle TWmap is robust for small parameter perturbation of s. Note that the TWmap based on chaotic map is very sensitive for small parameter perturbation [1]. Characteristics of ω is shown in Fig. 6 (b) which has more step than Fig. 6 (a).

If the parameter s varies, the TWmap causes various phenomena as shown in Fig. 7. Increasing s, periodic behavior is changed into chaotic behavior. Since the slope outside the window is 1, s can govern behavior of the TWmap : SSPOs for $s = 0$, periodic behavior for $0 < s < 1$, periodic
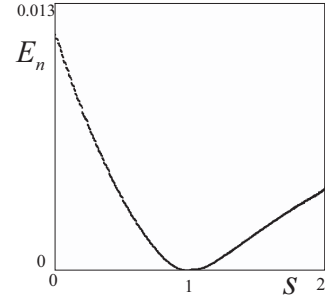

Figure 8: Characteristics of E_n for $\epsilon = 0.1$.
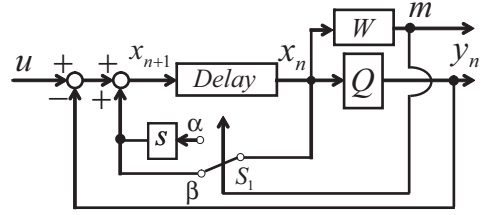

Figure 9: A block diagram of ADCs.

behavior/torus for $s = 1$ and chaos for $1 < s < \frac{1}{\epsilon}$. We then define E_n that is a deviation of the frequency ratio ω and parameter u :

$$E_n = \int_0^1 |u - \omega| du. \tag{5}$$

Fig. 8 illustrates characteristics of E_n for s. We can see that E_n decreases as s approaches 1. If $s = 1$, the TWmap is equivalent to the circle map and ω can take all rational number. It should be noted that behavior of the circle TWmap is stable if $s < 1$, but unstable if $s > 1$.

4. Application of the TWmap to ADCs

In this section, we present an application of the TWmap to ADCs. Fig. 9 shows a block diagram of the ADCs and its dynamics is described by Eq. (2) where dynamic range $I_2 \equiv [u - 1, u]$. Q denotes a 1-bit quantizer where $x_c \equiv 0$. u and y_n denote an analog dc input and a digital output sequence, respectively. If W does not exist, the system becomes basic ADC [11] where switch S_1 connects to node β at all the time. It should be noted that the ADC operates within finite time n up to the code length l. The ADC converts an analog dc input u into digital output sequence $(y_1, \cdots, y_l)$ and an approximation is given by integration: $\tilde{u} \equiv \frac{1}{l} \sum_{n=1}^{l} y_n$. Fig. 10 (a) and (c) show typical operation and Fig. 11 (a) shows conversion characteristics.

Applying the window W to the ADC, we obtain ADCs with a trapping window [6]. If x_n enters W, S_1 is connected to the node α and the operation finishes at trapping time m. The ADC outputs digital output sequence $(y_1, \cdots, y_m)$ for input u where m is determined by the window size ϵ and the approximation is given by $\tilde{u} = \frac{1}{m} \sum_{n=1}^{m} y_n$. For simplicity,
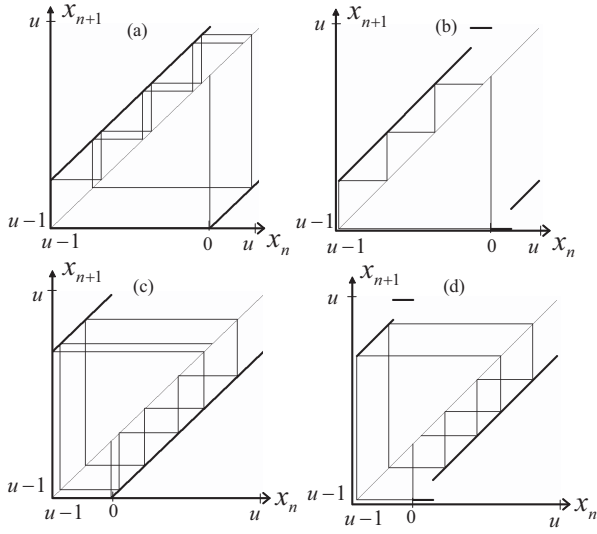
Figure 10: Behavior of the ADCs for $l = 9$. (a) Basic ADC for $u = 0.24$ and $\tilde{u} = \frac{2}{9}$, (b) ADC with a trapping window for $u = 0.24$, $\epsilon = 0.1$ and $\tilde{u} = \frac{1}{4}$. (c) Basic ADC for 0.72 and $\tilde{u} = \frac{6}{9}$, (b) ADC with a trapping window for $u = 0.72$, $\epsilon = 0.1$ and $\tilde{u} = \frac{5}{7}$.
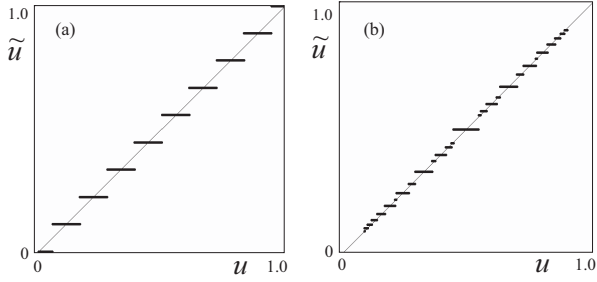

Figure 11: Comparison with conversion characteristics for $l = 9$. (a) Basic ADC, (b) ADC with a trapping window for $\epsilon = 0.1$ and $s = 0$.

we assume the following conditions :

$$\epsilon < u < 1 - \epsilon, \quad 1 < m \le l, \quad \frac{1}{\epsilon} - 1 \le l, \quad s = 0, \qquad (6)$$

and let initial state $x_1 \equiv 0$. Fig. 10 (b) and (d) show typical operation and Fig. 11 (b) shows conversion characteristics. Operation of the ADC without the window finishes with fixed time l and $\tilde{u}$ is given a fraction with fixed denominator l. On the other hand, ADC with the window finishes within $m \le l$ and $\tilde{u}$ is given a fraction with variable denominator: it can realize higher resolution as suggested in Fig. 10. Note that the circle map for irrational rotation numbers has quasi-periodic orbits with zero Lyapunov exponent in the steady state. The circle TWmaps behave periodic orbits even if parameter perturbation occurs as shown in Fig. 4 and Fig. 5: ADCs with a trapping window has more robustness than basic ADC.

5. Conclusions

We have presented the TWmap and consider its SSPOs. When a slope parameter on the window varies, the TWmap exhibits various phenomena. The slope can control behavior of the TWmap. The TWmaps are related to ADCs with a trapping window and it can realize higher resolution and stronger stability than basic ADCs. Future problems include detailed analysis of bifurcations and application to various practical systems.

References

[1] Y. Matsuoka, H. Torikai and T. Saito, "Chaotic Superstable Periodic Orbits in Nonlinear Circuits," *Proc. ICSES*, pp. 67-70, 2006.

[2] T. Saito, F. Komatsu and H. Torikai, "Superstable synchronous phenomena of switch-coupled relaxation oscillators," *IEICE Trans. Fund.*, 85, 10, pp. 2318-2325, 2002.

[3] Y. Matsuoka and T. Saito, "Rich Superstable Phenomena in a Piecewise Constant Nonautonomous Circuit with Impulsive Switching," *IEICE Trans. Fund.*, 89, 10, pp. 2767-2774, 2006.

[4] M. Shimazaki, H. Torikai and T. Saito, "Synchronization and Window Map from Pulse-Coupled Relaxation Oscillators," *IEICE Tran., Fund.*, 87, 9, pp. 2426-2431, 2004.

[5] C. Wagner and R. Stoop, "Renormalization Approach to Optimal Limiter Control in 1-D Chaotic Systems," *J. Statistical Physics*, 106, pp. 97-107, 2002.

[6] T. Saito and H. Imamura, "Analysis of a simple A/D converter with a trapping window," *Proc. of IEEE / ISCAS*, III, pp. 626-629, 2003.

[7] T. Saito, T. Kabe, Y. Ishikawa, Y. Matsuoka and H. Torikai, "Piecewise constant switched dynamical systems in power electronics," *International Journal of Bifurcation and Chaos*, 2007 (accepted).

[8] K. Matsumoto and I. Tsuda, "Noise-Induce Order," *J. Statistical Physics*, 31, pp. 87-106, 1983.

[9] S. Doi, "A Chaotic Map with a Flat Segment Can Produce a Noise-Induced Order," *J. Statistical Physics*, 55, pp. 941-964, 1989.

[10] R. M. Gray, "Oversampled sigma-delta modulation," *IEEE Trans. Commun.*, 35, 5, pp. 481-489, 1987.

[11] S. Hein and A. Zakhor, "New Properties of Sigma-Delta Modulators with dc Inputs," *IEEE Trans. Circuit. Syst.*, I, 40, 8, pp. 1375-1387, 1992.

[12] A. Teplinsky, E. Condon and O. Feely, "Driven Interval Shift Dynamics in Sigma-Delta Modulators and Phase-Locked Loops," *IEEE Trans. Circuit. Syst.*, I, 52, 6, pp. 1224-1235, 2005.